DOI: 10.1002/chem.200601878

A Bioorganometallic Approach for the Electrochemical Detection of Proteins: A Study on the Interaction of Ferrocene–Peptide Conjugates with Papain in Solution and on Au Surfaces

Khaled A. Mahmoud and Heinz-Bernhard Kraatz*[a]

Abstract: In this paper, a new bioorganometallic approach for the detection of proteins using surface-bound ferrocene–peptide conjugates is presented. Specifically, a series of peptide conjugates of 1′-aminoferrocene-1-carboxylic acid (ferrocene amino acid, Fca) is synthesized: Boc-Fca-Gly-Gly-Tyr(Bzl)-Arg(NO_2)-OMe (**2**), Thc-Fca-Gly-Gly-Tyr(Bzl)-Arg(NO_2)-OMe (**3**), Thc-Fca-Gly-Gly-Tyr(Bzl)-Arg(NO_2)-OH (**4**), Boc-Fca-Gly-Gly-Arg(Mtr)-Tyr-OMe (**7**), Thc-Fca-Gly-Gly-Arg-(Mtr)-Tyr-OMe (**8**), Thc-Fca-Gly-Gly-Arg(Mtr)-Tyr-OH (**9**), Thc-Fca-Gly-Gly-Arg-Tyr-OH (**10**). The peptide is conjugated to the C-terminal side of Fca and compounds **4**, **7**–**10** possess a thiostic acid linked to the N-terminal side of Fca in order to facilitate formation of thin films on gold substrates. Competitive inhibition towards papain was determined for Thc-Fca-Gly-Gly-Tyr(Bzl)-Arg(NO_2)-OH (**4**), Thc-Fca-Gly-Gly-Arg(Mtr)-Tyr-OH (**9**) and Thc-Fca-Gly-Gly-Arg-Tyr-OH (**10**). The binding interaction between the peptide modified substrates and papain enzyme was studied using real-time surface plasmon resonance (SPR) imaging. Peptide **10** showed the strongest binding affinity to papain. Adsorption/desorption rate constants were $k_a = 1.75 \pm 0.05 \times 10^5\,\text{M}^{-1}\text{s}^{-1}$ and $k_d = 2.90 \pm 0.05 \times 10^{-2}\,\text{s}^{-1}$. Interactions of papain with Fca–peptide **10** were investigated by cyclic voltammetry. The interaction results were also verified by measuring the electrochemical response of the peptide–papain interaction as function of increasing enzyme concentration. A linear relationship was observed for papain concentration of up to 80 nM. Shifting to higher potentials as well as decrease in the overall signal intensity was observed. The detection limit was 4×10^{-9} M.

Keywords: biosensor · electrochemistry · enzymes · ferrocene · peptides

Introduction

Enzymatic transformations of substrates are often exploited for the development of amperometric sensors. The electrochemical sensors have received a major attention in the biosensing technology, in particular the use of glucose oxidase for the development of an electrochemical glucose sensitive detector.[1–7] The resulting devices exploiting this technology are simple to use, inexpensive and accurate. More importantly, they are amenable to miniaturization and hence the design of high-density arrays.[8]

The detection of biomolecular interactions by electrochemical methods requires in general the presence of a redox-active probe as part of the detection system (Scheme 1). The redox probe can be in solution or can be covalently attached to the molecule capturing the biomolecule from solution. In both cases, the interaction of the surface with the biomolecule will alter the electron-transfer properties of the systems. For solution-based redox probes, significant differences exist in the electron-transfer properties or ability of the redox probe and/or counter ions to diffuse into the film (Scheme 1a). These differences can be exploited for the detection of protein binding to a range of capture probes. In essence, this approach is "label-free", since no chemical modifications of the capture probe or of the target protein are necessary.[9,10] An interesting variation on the theme of a solution-based electroactive probe is the use of a redox-active polymer. Using a ferrocene (Fc)-labeled polythiophene which electrostatically binds to duplex DNA or duplex DNA–PNA), it was possible to detect thrombin.[10–13] More recently, electrochemical immunoas-

[a] K. A. Mahmoud, Prof. H.-B. Kraatz
Department of Chemistry, University Of Saskatchewan
110 Science Place, Saskatoon, SK S7N5C9 (Canada)
Fax: (+1) 306-966-4730
E-mail: kraatz@skyway.usask.ca

Supporting information for this article is available on the WWW under http://www.chemeurj.org/ or from the author.

says (EIA) were developed in which an analyte binds to an immobilized antibody, followed by binding of a redox mediator bound to an antibody which binds to the electrode-bound analyte (Scheme 1b).[14,15] In cases where the redox probe is covalently attached to a terminal position of a molecule such as single stranded DNA, the interaction with the appropriate target will result in large structural changes of the capture probe causing changes in the electron transfer kinetics of the system. Heeger's DNA-hairpin loop is an example for this approach (Scheme 1c).[16] In the absence of a suitable target, an Fc probe attached to the 5′-position in a single-stranded DNA is in close proximity to the electrode surface and gives rise to a significant redox response. Upon hybridization of a target strand to the (Fc)-labeled capture strand, significant structural changes occur which change the distance between the Fc group and the surface, resulting in a decrease of the electrochemical response. Although this approach is useful in cases of DNA–DNA or DNA–protein detection where the interaction does not involve the site of the redox probe,[17] it will have limited utility for monitoring peptide–protein interactions. In this case, the presence of a terminal redox probe may significantly interfere with the interaction and may even prevent it.

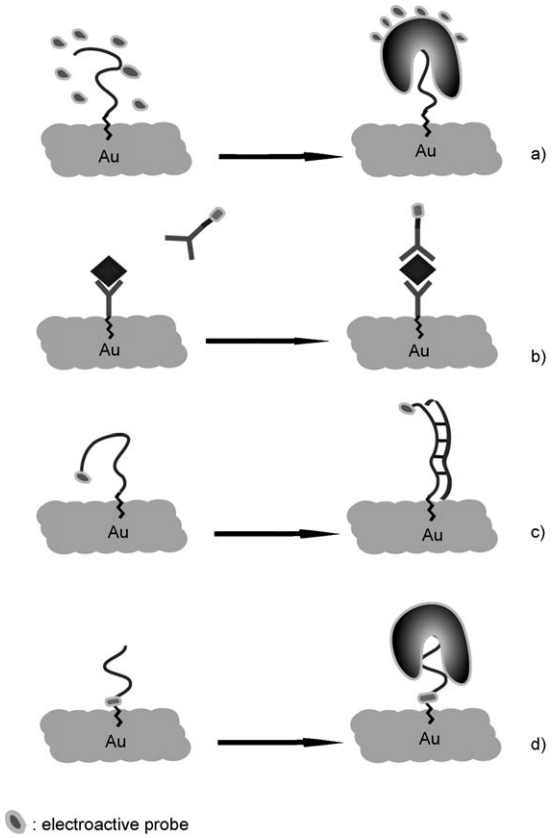

Scheme 1. Schematic representation of some of the common electrochemical biosensor systems (a–c) and the new proposed system making use of an ferrocene–peptide conjugate (d): a) Redox active probe in solution and the target protein blocks its interaction with the surface. b) In the electrochemical immunoassay (EIA) a protein binds to a surface-bound capture probe followed by binding labeled antibody. c) Conformational changes take place upon binding of a target DNA to a single stranded capture DNA. Changes in the distance between the redox label and the surface alter the electrochemical behavior of the system. d) Bioorganometallic capture probe: protein binding is detected by monitoring the electrochemical properties before and after protein binding.

We are proposing a new approach making use of our expertise in bioorganometallic chemistry to join a peptide recognition sequence to a redox probe. The idea is that a surface-bound redox probe is in close proximity to the electrode surface and thus unaffected by diffusive processes. Interaction between the recognition sequence and electrode surface will not be hindered by the interaction with the target analyte. This in turn may enhance the sensitivity and may render a potential device less susceptible to environmental influences.

Fc–peptide conjugates are an attractive class of organometallic peptide conjugates that are conveniently obtained by solution or solid-phase synthetic strategies,[18] that have the potential to be tailored to target DNA and specific proteins.[19–22] In a recent study, it was demonstrated that 1′-aminoferrocene-1-carboxylic acid (ferrocene amino acid, Fca) induces a turn into a peptide sequence and thereby allows control over the peptide secondary structure.[23] Recently, Rapić et al. and Heinze et al. independently used solid-phase peptide synthesis (SPPS) to obtain Fca-oligopeptides by combining Fmoc and Boc procedures.[24,25]

In this contribution, we outline how Fca–peptide conjugates can be used in protein detection and demonstrate our approach for the detection of papain, which is a cysteine protease commonly found in the papaya fruit and used commercially as a meat tenderizer. In our approach (see Figure 1d), a thin film on gold prepared from a conjugate of Fca with an inhibitory peptide sequence to papain is used for the detection of papain. We are reporting the results of a combined synthetic, spectroscopic and electrochemical study into the properties of these films and their behavior in the presence of papain.

Results and Discussion

Synthesis: In an early report, it was shown that the organometallic peptide conjugate Fc-Gly-Gly-Tyr-Arg interacts with papain and acts as a competitive inhibitor.[22] Based on this result, we decided to work with two peptide systems, making use of conjugation of Fca while exploiting the papain-binding sequence Gly-Gly-Tyr-Arg and Gly-Gly-Arg-Tyr. Conjugation of the tetrapeptide to the C-terminal side of Fca will allow the interaction with the protein, while the N-terminal side will be exploited to surface binding of the Fca conjugate. The synthesis of Fca–peptide conjugate **4** was achieved by carbodiimide coupling in solution and is summarized in Scheme 2. Compound **4** displayed a broad band in the IR spectrum assigned to the OH stretch and the expected carbonyl stretch for the acid group at 1741 cm^{-1}. Unfortunately, it was not possible to deprotect the guanidine group of peptide conjugate **4** by hydrogenation, presumably

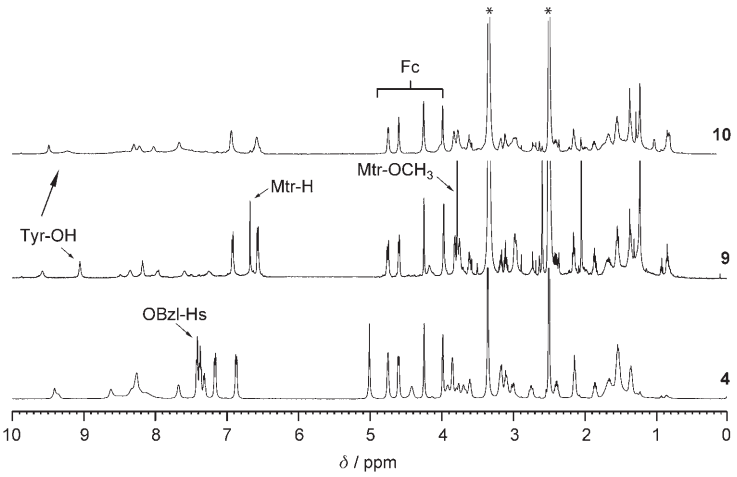

Figure 1. ^{1}H NMR of peptides **4**, **9**, and **10**. * [D_5]DMSO trace at $\delta = 2.50$ ppm, water trace at $\delta = 3.33$ ppm.

a result of Pd catalyst poisoning caused by the thiostic acid (Thc) disulfide group. In order to overcome this problem, we decided to implement a small positional change in the sequence involving the Tyr and Arg, which facilitated the synthesis and did not require protection of the Tyr. The Arg guanidine group was protected by Mtr, which could be deprotected with TFA and thioanisole. The synthesis of Fca–peptide conjugates **9** and **10** is summarized in Scheme 3.

The peptide building block **6** was synthesized from Boc-Gly_2-OH and the corresponding dipeptide H-Arg(Mtr)-Tyr-OMe (**5**). Boc deprotection and conjugation to the carboxylic acid group of Fca resulted in the desired conjugate **7**. After Boc deprotection of the amino group of Fca under anaerobic conditions, Thc-conjugate **8** was formed. Stepwise deprotection of the methyl ester by hydrolysis and of the Mtr group by TFA/anisole resulted in the formation of compound **9** and **10**, respectively. Final purification of compound **10** was carried out by HPLC. The identity of compounds **9** and **10** was confirmed by full spectroscopic analysis including ToF-MS, IR and ^{1}H NMR spectroscopy. In the IR compounds **9** and **10** showed amide-A bands at 3306 and 3447 cm^{-1}, respectively and carbonyl stretch at 1748 and 1725 cm^{-1}, respectively. Figure 1 shows the ^{1}H NMR spectra in [D_6]DMSO for the main three peptides **4**, **9**, and **10** under investigation. In all three peptides, the amide as well as guanidine protons were observed in the region $\delta =$ 8.6–7.3 ppm. The peaks assigned for Mtr protecting group in peptide **9** disappeared in peptide **10** indicating the successful deprotection.

Inhibition studies: Before linking the Fca–peptide conjugates onto a gold surface, it was important to evaluate the Fca conjugates for their ability to inhibit papain in solution. For this purpose, papain was assayed with the chromogenic substrate Z-Phe-Arg-NHNp in the absence and presence of the Fca–peptide conjugates **4**, **9** and **10**. The Michaelis–Menten constant (K_m) for papain as well as the inhibition constant K_i for the peptides were determined. The K_m value was determined by monitoring the total papain-catalyzed

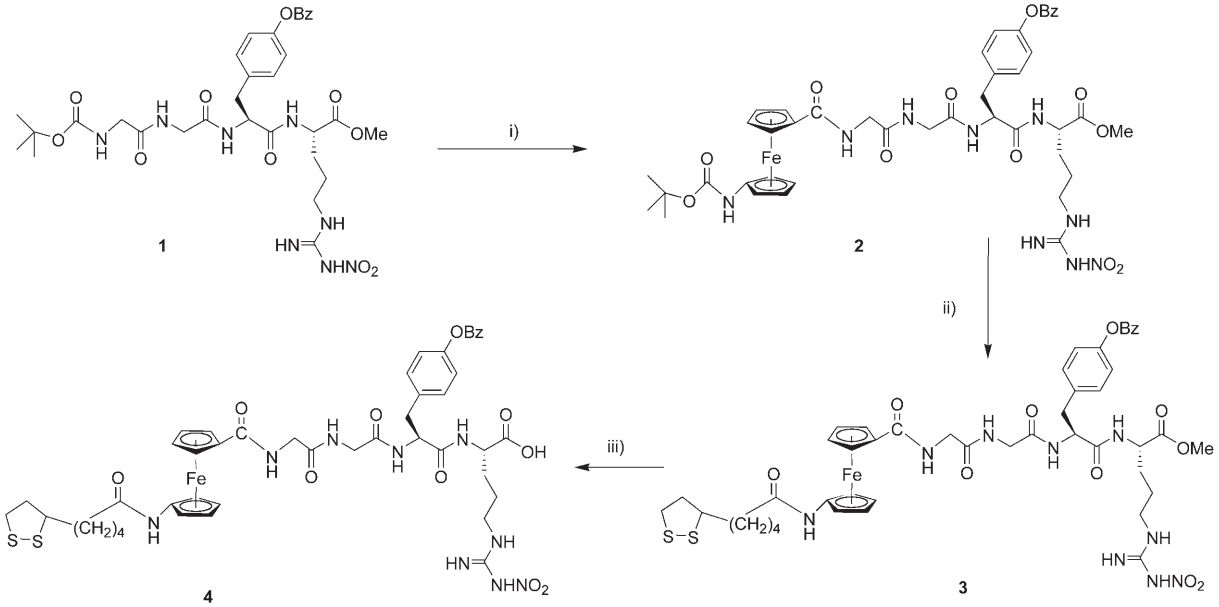

Scheme 2. Synthesis of Fca–peptide conjugate **4**. i) TFA/CH_2Cl_2; Boc-Fca-OBt; Et_3N, CH_2Cl_2; ii) TFA/CH_2Cl_2; ThcOH, EDCI/HOBt; Et_3N, CH_2Cl_2; iii) NaOH/CH_3OH/H_2O. EDCI·HCl = 1-ethyl-3-(3-dimethylaminopropyl)carbodiimide hydrochloride.

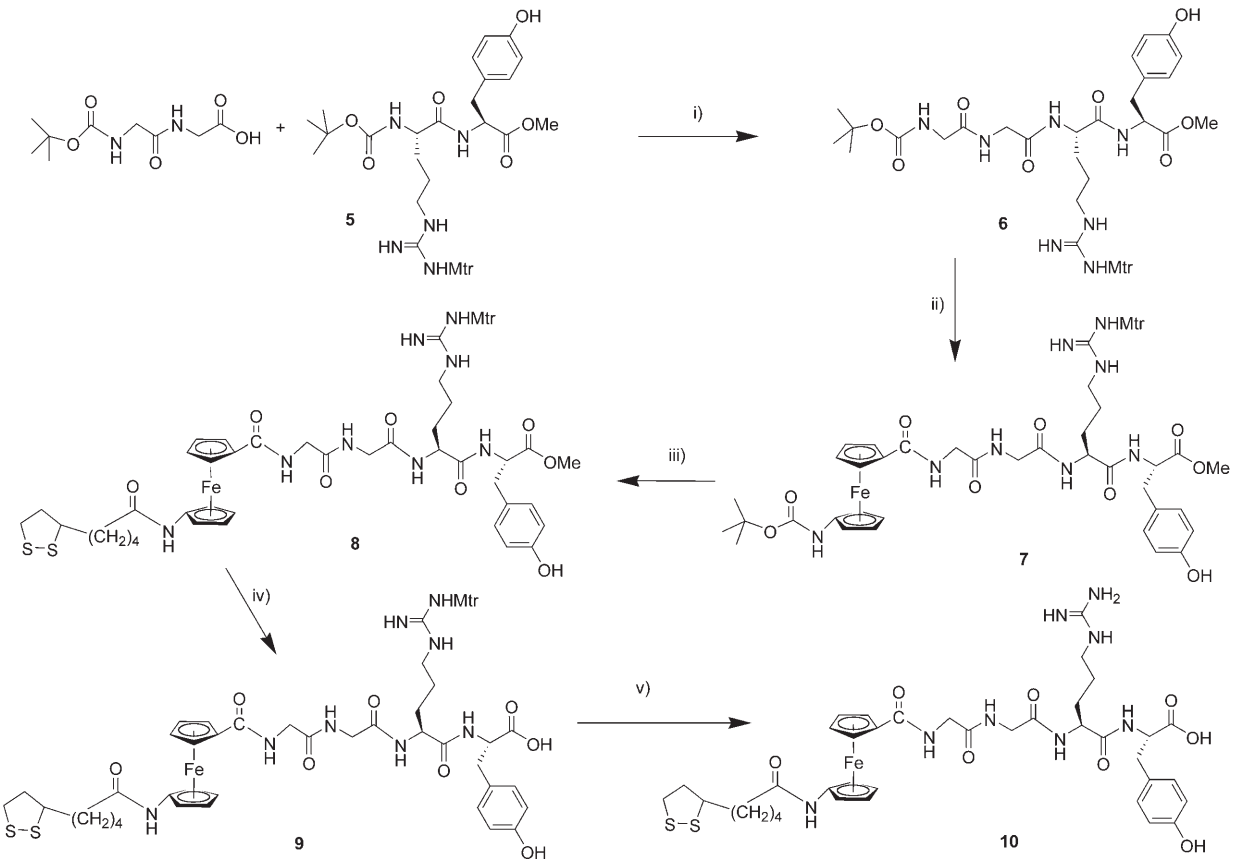

Scheme 3. Synthesis of Fca–peptide conjugates **7**–**10**. i) TFA/CH_2Cl_2; EDC/HOBt; Et_3N/CH_2Cl_2; ii) TFA/CH_2Cl_2; Boc-Fca-OBt; Et_3N/CH_2Cl_2; iii) TFA/CH_2Cl_2; ThcOH/EDC/HOBt; Et_3N/CH_2Cl_2; iv) NaOH/CH_3OH; v) TFA/thioanisole/CH_2Cl_2.

hydrolysis of Z-Phe-Arg-NHNp in the absence of the inhibitors and at high initial concentration of the substrate. A K_m value of 980 ± 26 μM was determined at pH 6.2 by nonlinear regression fit of the concentration velocity curve using Michaelis–Menten equation ($\vartheta = \vartheta_{max}[S]/(K_m + [S])$, where ϑ is the velocity and ϑ_{max} is the maximum velocity, and [S] is the substrate concentration (Supporting Information, Figure S2). The value compared well with the previously reported one of 965 ± 244 μM.[26] A representative kinetic analysis of papain inhibition by the two Fca–peptide conjugates **9** and **10** is shown in Figure S3 of the Supporting Information. The Dixon–Webb plots indicate a time-independent inhibition. The slopes of the progress curves were directly used to determine K_i' value, from which K_i value was calculated to be 210 ± 1.4 μM for compound **9** and 6.9 ± 0.2 μM for compound **10**. Our results suggest that these Fca–peptide conjugates exhibit competitive inhibition behavior.[26] The inhibition constants for **10** indicates very good competitive inhibition of papain, comparable to that of the Fc-conjugate Fc-Gly-Gly-Try-Arg-OH, which has a $K_i = 9$ μM at pH 6.2 (Table 1).[27]

On the other hand, lower affinities were observed for the Fca–peptide conjugates **4** ($K_i = 820.9 \pm 2.5$ μM) and **9** ($K_i = 210 \pm 1.4$ μM), which is rationalized by the presence of protecting groups which may not allow a proper interaction with Cys25 and His159 in the active site of papain.[29–31] It is

Table 1. Inhibition constant K_i of the Fc–peptide conjugates **4**, **9**, and **10** and some literature compounds.

Compound	pH	K_i' [μM]	K_i [μM]	Ref.
4	6.2	2510.6 ± 8.8	820.9 ± 2.5	this work
9	6.2	639.1 ± 1.1	210 ± 1.4	this work
10	6.2	21.1 ± 0.3	6.9 ± 0.2	this work
$Gly_2TyrArg$	6.0		150	[27]
$Gly_2Tyr(Bz)Arg$	6.0		123	[28]
Fc-$Gly_2TyrArg$	6.2		9	[22]

interesting to note that switching the peptide sequence from the original sequence employed by Kaiser for purification of papain by affinity chromatography Gly-Gly-Tyr-Arg[28] to Gly-Gly-Arg-Tyr, the peptide became a more potent inhibitor. Blumberg[27] and Kaiser[28] used Gly-Gly-Tyr(Bzl)-Arg for the purification of papain by affinity chromatography. It was shown that papain inhibition can be achieved by peptides that have Arg and an aromatic amino acid in the P_1 and P_2 subsites (nomenclature according to Schechter and Berger,[32] see Supporting Information Figure S4). It was found that the peptide sequence Z-Arg-Leu-Val-Gly-DAM gave the most potent inhibitor of papain with apparent second order rate constants of the same order of magnitude as those determined for {1-[*N*-[(L-3-*trans*-carboxyoxirane-2-carbonyl)-L-leucyl]amino]-4-guanidinobutane} E-64, the

most common inhibitor of cysteine proteases.[33] Moreover, a strong electron-withdrawing phenyl groups at the C-terminus constructs a good irreversible inhibitor for papain.[34] Crystal structures of related papain–inhibitor complexes showed that the inhibitor extends along the S_n ($n=1\approx2$) subsites of the enzyme and is stabilized in the active-site groove by a series of hydrogen bonds and hydrophopic interactions which may have higher priority than the P–S interactions.[34–36] Based on X-ray structures showing the interaction of inhibitor molecules with papain, it is proposed that our inhibitor interacts with His158, Gly66, Asp158 and Gln19 (Figure 2).[34,36,37] Despite the recent results obtained

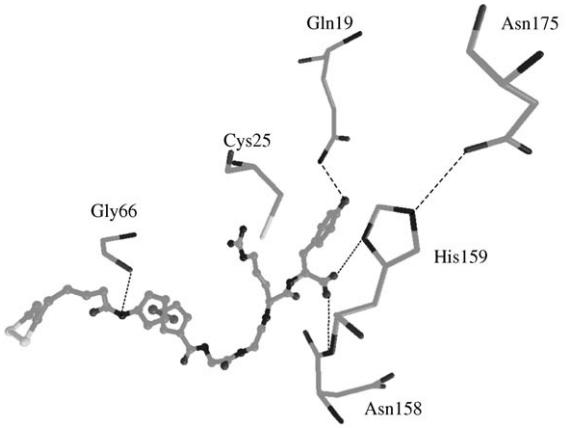

Figure 2. Proposed structure of peptide **10** interacting with the binding site of papain. The initial enzyme–inhibitor structure was modeled in the VEGA ZZ 2.0.5 program[38] based on the papain structure **1PE6** studied by Yamamoto et al.[36] The papain–peptide complex model was constructed by replacing the inhibitor in structure **1PE6** with peptide **10** as the chosen inhibitor in our case. The initial geometry of peptide **10** and papain–peptide complex were modeled by energy minimization using molecular mechanics calculation method (MM) in Spartan. The enzyme–inhibitor complex distances were in good agreement with X-ray crystallographic studies.[36]

by Gütschow[26] that papain prefers aromatic residues over aliphatic ones in the P_2 position, the structural basis of this argument was not clearly addressed. It appears that the binding pocket is more flexible with regards to molecular recognition. Peptide **10** possesses Arg in P_2 and Tyr in P_1 and exhibits good molecular recognition properties. The new sequence Thc-Fca-Gly-Gly-Arg-Tyr exhibits the strongest inhibition of papain, $K_i=6.9\pm0.2$ μM. Presumably, N-conjugation of the inhibitory sequence with Thc-Fca residues enhances the affinity for papain binding site.[22] As was demonstrated earlier in solution studies on the Fc derivative (Fc-Gly-Gly-Tyr-Arg),[22] the organometallic Fca group is most likely encapsulated, which appears to enhance the interaction with the protein.

SPR Imaging: The next step in this investigation was to determine the potential of the Fca–peptide conjugates to be active towards papain binding when linked on a surface. This will allow us to evaluate the formation of the peptide–protein complex on the surface and is a useful step towards the evaluation of the interaction by electrochemical methods. The idea was to exploit the Thc disulfide of conjugates **4**, **9**, and **10** for binding to a gold surface. The resulting Fca–peptide film will have the Fca groups firmly embedded in the film and the inhibitory peptide exposed allowing papain to bind. SPR imaging was selected as a method of choice because of its powerful ability to study the bioaffinity interactions thin films on gold.[39–42] The quantitative measurements of papain interactions with the Fca–peptide modified surface by SPR imaging allowed to measure the change in the percentage reflectivity ($\Delta\%\ R$) which was directly proportional to the fractional surface coverage θ of the peptide-modified surface by papain, providing $\Delta\%\ R$ is below 10%.[43] Using this method, the adsorption and desorption kinetics of papain were determined. Peptides **4**, **9** and **10** were immobilized on spot ready SPR microchips by spotting ethanolic solutions of the conjugates onto the four gold pads each per chip and then monitored the selective binding to papain by real-time SPR imaging, as described in the Experimental Section (Figure 3). This was achieved by monitoring changes in percentage reflectivity as a function of papain concentration (up to 200 nM) under continuous flow. Conjugate **10** exhibited a significantly higher change in $\Delta\%\ R$ compared with the other two conjugates **4** and **9**. This was in agree-

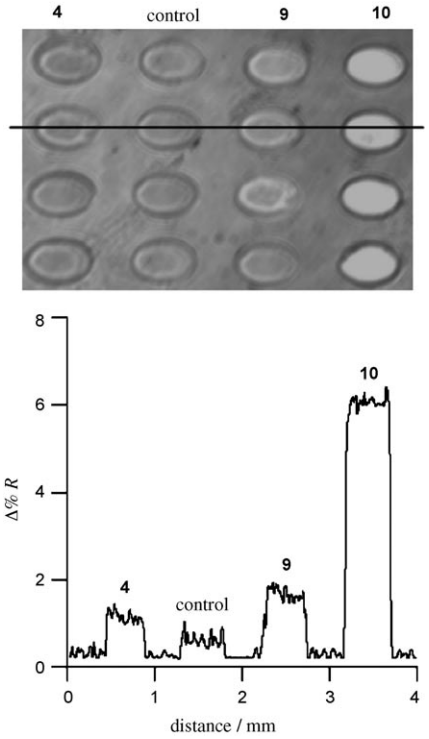

Figure 3. SPR imaging measurements showing the interaction of papain (150 nM) with surface-bound Fca–peptide conjugates **4**, **9**, and **10** and a decanethiol control. Papain was dissolved in a buffer solution (0.1 M sodium phosphate pH 6.2, 2.5 mM EDTA, 300 μM DTT, and 30% DMSO, 23 °C. a) SPR difference image resulting from subtraction of the buffer image from the ones obtained after interaction with papain. b) Line profile, taken across the difference images, shows significant differences in the $\Delta\%\ R$ for measurements taken in the absence and presence of papain.

ment with the solution studies (see above). Figure 4 shows the increase in $\Delta\%\ R$ due to papain–surface interaction. The binding curve reaches a steady state when papain adsorption and desorption rates were equal. At this point,

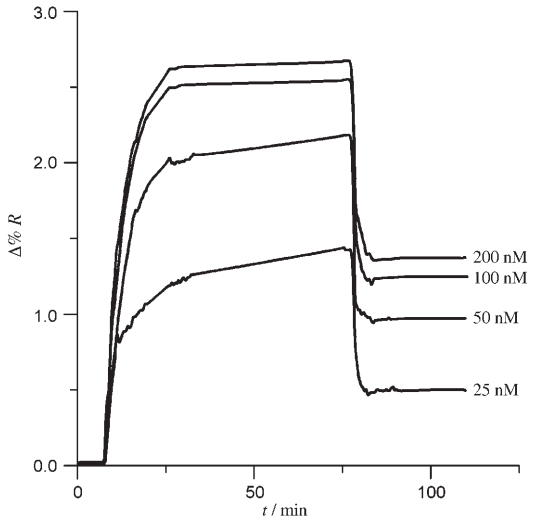

Figure 4. Plot of $\Delta\%\ R$ versus time for the interaction of papain with thin films of Fca–peptide conjugate **10** on gold. The concentration of papain was increased from 25–200 nM.

papain-free buffer was injected and flowed over the peptide array. In order to extract values for the association (k_a) and dissociation (k_d) rate constants, sequential fitting of the response curves over a series of different protein concentrations was required. Assuming a 1:1 interaction model between papain and the surface-bound Fca–peptide, Equation (1) was used to determine the rate of desorption.

$$\Delta\%\ R(t) = \Delta R \exp(-k_d t) \quad (1)$$

The adsorption curves are determined using a simplified Langmuir isotherm by:

$$\Delta\%\ R(t) = \Delta R\,(1-e^{\gamma t}) \quad (2)$$

where $\gamma = k_a c + k_d$ with c being the protein concentration. ΔR can also be defined as equal to the product $\Delta R_{max}\theta$, where ΔR_{max} is the maximum SPR signal obtained when all surface binding sites are occupied and θ is the fraction of the total surface coverage. Figure 5 shows a plot of γ versus papain concentration by fitting the adsorption curves shown in Figure S5, Supporting Information, to Equation (2). $k_a = 1.75 \pm 0.05 \times 10^5\ M^{-1}\ s^1$ and $k_d = 2.90 \pm 0.05 \times 10^{-2}\ s^{-1}$ were obtained from the slope and intercept, respectively. Moreover, the equilibrium adsorption constant $K_{ads} = 6.03 \times 10^6\ M^{-1}$ was obtained from the ratio of k_a and k_d.

The K_{ads} value was within the reported range of binding constants for the interaction between proteins with immobilized peptides from $1.7 \times 10^6\ M^{-1}$ to 1.5×10^8.[42,44–47]

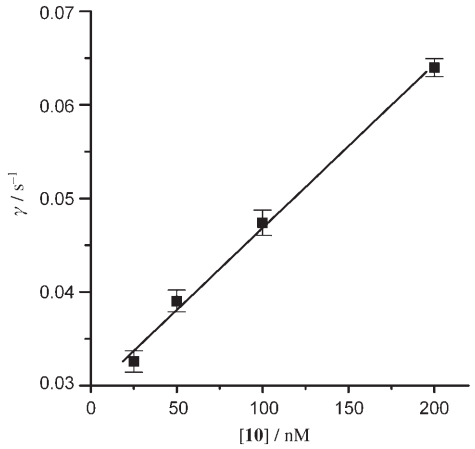

Figure 5. Plot of γ versus papain concentration for conjugate **10** obtained from fitting the adsorption curves to Equation (2). The linear slope corresponds to the adsorption rate constant $k_a = 1.75 \pm 0.05 \times 10^5\ M^{-1}\ s^1$ and the y intercept corresponds to the desorption rate constant $k_d = 2.90 \pm 0.05 \times 10^{-2}\ s^{-1}$.

Electrochemistry: Fca–peptide conjugates **10** displayed the lowest inhibition constant in solution and also performed well when present as a thin film. Next, we decided to test our major hypothesis of the new label-based electrochemical detection and exploit the redox activity of the Fca group to detect the binding of papain to the inhibitory peptide sequence in conjugate **10**. The electrochemical studies were carried out using Fca–peptide films prepared on 25 μm gold microelectrodes. The peptide films were prepared by immersing the microelectrodes in Thc-terminated peptides prepared in 5% (by volume) acetic acid in ethanol at concentration of approximately 1 mM for 36 h. As described in Scheme 1d the Fca label is located at the base of the peptide capturing layer allowing direct connection and close proximity to the gold surface.

Under these conditions, the disulfide-containing Thc group adsorbed to the gold surface involving a stable Au–S linkage.[48,49] The next step involved the dilution of the Fca–peptide in order to close available pinholes present in the film and cover any solution accessible gold. The dilution was carried out by immersing the Fca–peptide-modified gold microelectrodes in an ethanolic solution of decanethiol (0.5 mM) for about two minutes. The electrochemical response of the films was evaluated by cyclic voltammetry (CV) measurements in papain activation buffer at pH 6.2 containing $NaClO_4$ (2 M) as supporting electrolyte. Measurements were repeated for ten separate microelectrodes in order to obtain statistically meaningful results. The films exhibited a single fully reversible one-electron redox peak with a formal potential E^0 of 0.459 ± 0.005 V at a scan rate of $10\ V\,s^{-1}$ versus Ag/AgCl. Figure 6 shows the change of the CV as a function of increasing papain concentration.

As the enzyme concentration increased, the formal potential of the Fca probe was shifting to higher potentials, indicating that oxidation of the Fca group became increasingly more difficult as papain was binding to the inhibitory pep-

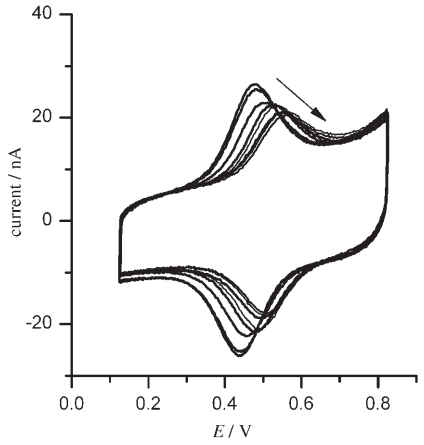

Figure 6. Cyclic voltammogram of 25 μm diameter gold microelectrodes modified with a mixed film of Fca–peptide **10** and decanethiol in the presence of increasing concentrations of papain (The arrow direction indicates a signal decrease and shift to higher potential with increasing the concentration from 0 to 200 nM). Enzyme activation buffer (0.1 M sodium phosphate pH 6.2, 2.5 mM EDTA, 300 μM DTT, and 30% DMSO, 23 °C) with 2 M $NaClO_4$. Scan rate of 10 $V s^{-1}$, Pt counter, Ag/AgCl reference.

tide. In case of the Fc derivative Fc-Gly-Gly-Tyr-Arg, these changes were caused by slight changes in the chemical environment around the Fc group.[22] This change is illustrated in Figure 7, which shows a plot of E^0 as a function of papain

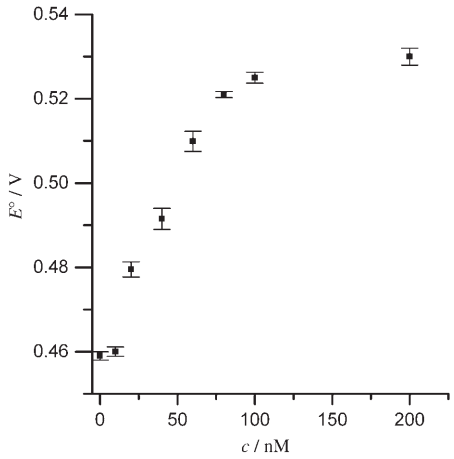

Figure 7. Plot of the formal potential (E^0) vs papain concentration.

concentration. A linear relationship was observed for papain concentration of up to 80 nM, after this concentration the potential reaches a steady state indicating potentially the saturation of the surface with papain. The detection limit was 4×10^{-9} M, estimated from $3(S_b/m)$, where S_b is the standard deviation of the measurement signal for the blank and m the slope of the analytical curve in the linear region.[50]

In addition, a small decrease in the overall signal intensity was observed, most likely as a result of less efficient penetration of the film by the supporting electrolyte, thereby decreasing the ability of the Fca to be oxidized. However, we do not loose the ability to detect the interaction between the peptide and the protein. In contrast to our observations, in some cases severe problems can occur that will result in the loss of signal. In Katayama's sensor system,[9] a significant reduction in current was observed as a function of c-AMP addition to the system, ultimately leading to loss of signal at high c-AMP concentrations. It is likely that these changes are caused by decreased access of the $[Fe(CN)_6]^{3-/4-}$ redox probe to the surface. In aptamer-based systems, the aptamer is highly dynamic in the absence of the target analyte allowing efficient electron transfer between the redox tag and the surface. The electron transfer is affected by analyte binding and in some cases even inhibited.[51–54]

In order to gain further support for the interaction of papain with films of conjugate **10**, measurements were carried out involving a quartz crystal microbalance. For this purpose, peptide films were immobilized on the gold pad on the quartz crystals following the identical procedure used for gold microelectrodes. In the QCM measurements, changes in the frequency are monitored as a function of time as depicted in Figure 8. In the presence of the blank activation buffer solution only continuous decay of Δf was observed, most likely caused by buffer migration. In the presence of papain, the protein adsorbs to the film of conjugate **10** and after some time reaches steady state. The change in frequency Δf before and after papain addition is 34.1 ± 3 Hz, which is converted into a mass change using the Sauerbrey equation [Eq. (5)]. The average mass of papain adsorbed to the surface was 245 ± 3 ng cm^{-2} or 1.62×10^{-12} mol cm^{-2}.

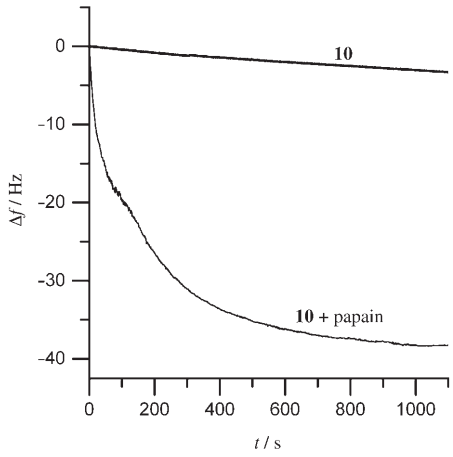

Figure 8. QCM measurement of papain adsorption on films of Fca–peptide conjugate **10** on gold covered AT-cut type crystals. Papain activation buffer: 0.1 M sodium phosphate pH 6.2, 2.5 mM EDTA, 300 μM DTT, and 30% DMSO, 23 °C with 2.0 M $NaClO_4$.

Conclusion

In summary, we have synthesized an bioorganometallic conjugate of Fca equipped with an inhibitory peptide sequence

that targets papain. Competitive inhibitions from solution assays and adsorption/desorption kinetics from real-time SPR imaging studies allowed the selection of peptide **10** as the most efficient capture probe for papain detection. The electrochemical measurements of surface-bound Fca–peptide **10** showed a significant electrochemical response of the sensor upon binding to papain. The signal is shifting anodically as well as decreasing in intensity, presumably due to the partial shielding of the Fca group by the papain. This represents proof of concept that our approach using bioorganometallic sensor systems provides an attractive alternative for the electrochemical detection of non-labeled non-redox active proteins, which under current detection schemes remains a significant challenge. Thus, the next step in our investigation is to optimize the sensor platform and expand out studies to include multiplexed measurements of several analytes by varying the recognition sequence on the Fca redox probe.

Experimental Section

Materials and general procedure: All syntheses were carried out under dry nitrogen gas unless otherwise indicated. CH_2Cl_2 (ACS grade) used for synthesis was dried (CaH_2) and distilled prior to use. $CDCl_3$ (Aldrich) was dried (CaH_2), and stored over molecular sieves (8–12 mesh; 4 Å effective pore size; Fisher) before use. THF was dried by distillation over benzophenone/sodium, and stored over molecular sieves (8–12 mesh; 4 Å effective pore size; Fisher) before use. 2-(1*H*-Benzotriazol-1-yl)-1,1,3,3-tetramethyluronium (HBTU), hydroxybenzotriazole (HOBt) (Nova), $MgSO_4$, and $NaHCO_3$ (VWR) were used as received. For column chromatography, a column with a width of 2.7 cm (ID) and a length of 45 cm was packed 18–22 cm high with 230–400 mesh silica gel (VWR). For TLC, aluminum plates coated with silica gel 60 F_{254} (EM Science) were used. NMR spectra were recorded on a Bruker Avance-500 spectrometer using a 5 mm broadband probe operating at 500.134 MHz (^{1}H) or 125.766 MHz (^{13}C{^{1}H}). Peak positions in the ^{1}H NMR spectra are reported in ppm relative to TMS. All otherwise it is described ^{13}C{^{1}H} spectra are referenced to the [D$_6$]DMSO signal at $\delta = 39.85$ ppm. Mass spectrometry was carried out on a VG Analytical 70/20 VSE instrument. Infrared spectra were recorded on a Perkin-Elmer model 1605 FTIR spectrometer. Analytical RP-HPLC for peptide 10 was performed on a Dionex HPLC system equipped with a Dionex Acclaim 3Lm C-18 (150×4.6 mm) column with a flow rate of 1 mL min^{-1}. Semipreparative RP-HPLC was performed on a Dionex HPLC system equipped with a Phenomenex Gemini 5Lm C-18 (250×10 mm) column with a flow rate of 2.0 mL min^{-1}. Mobile phase A was 0.1% TFA in water, mobile phase B was 0.1% TFA in acetonitrile. The gradiant was $t = 0$ min, B = 5%; $t =$ 20 min, B = 65%; $t = 25$ min, B = 90%; $t = 27$ min, B = 95%; $t = 27.1$ min, B = 8%; $t = 35$ min, B = 5%.

Papain, lyophilized powder ≥10 units per mg protein (E1%/280) and thiostic acid (Thc-OH) were purchased from Sigma. DTT (±-*threo*-2,3-dihydroxy-1,4-butanedithiol) was obtained from Fluka. Z-Phe-Arg-NHNP was purchased from Bachem, Bubendorf (Switzerland). The amino acid derivatives were purchased from Advanced ChemTech. Spot-ready SPR chips having sixteen 1 mm gold spots and plane gold SPR chips were purchased from GWC technologies. The syntheses of Boc-Gly-Gly-Tyr(Bzl)-Arg(NO$_2$)-OMe,[22] benzotriazol-1-yl-1′-(*tert*-butyloxycarbonylamino)ferrocene-1-carboxylate (Boc-Fca-OBt)[55] were described elsewhere.

Boc-Fca-Gly-Gly-Tyr(Bz)-Arg(NO$_2$)-OMe (2): Boc-Gly-Gly-Tyr(Bz)-Arg(NO$_2$)-OMe (**1**) (2.2 mmol, 1.54 g) was dissolved in CH_2Cl_2 and treated with TFA (3 mL) in CH_2Cl_2 (3 mL) for 30 min. The TFA and CH_2Cl_2 were subsequently removed in vacuo. The resulting residue was redissolved in CH_2Cl_2 and cooled in ice bath prior to the dropwise addition of Et_3N (0.45 mL). To this was added a solution of Boc-Fca-OBt (2 mmol, 0.92 g). The reaction mixture was then warmed to room temperature and left to stir overnight. Purification of the crude product was carried out by column chromatography on silica gel ($CHCl_3$/MeOH 90:10) to give yellow crystals of **2** (1.41 g, 76%). ^{1}H NMR ([D$_6$]DMSO) $\delta = 7.43$ (d, 2H, $J = 8$ Hz, Bz), 7.38 (t, 2H, $J = 9$ Hz, Bz), 7.32 (t, 1H, $J = 9$ Hz, Bzl), 7.15 (d, 2H, $J = 8$ Hz, Tyr-Bz), 6.89 (d, 2H, $J = 9$ Hz, Tyr-Bz), 5.05 (s, 2H, Tyr(O-CH$_2$)), 4.78 (s, 2H, H-2, H-5, Fc), 4.59 (s, 2H, H-2′, H-5′, Fc), 4.47 (m, 1H, Tyr(αCH)), 4.42 (s, 2H, H-3, H-4, Fc), 4.28 (m, 1H, Arg(αCH)), 4.06 (s, 2H, H-3′, H-4′, Fc), 3.71 (s, 2H, Gly^1(αCH)), 3.67 (s, 2H, Gly^2-(αCH)), 3.61 (s, 3H, COOCH$_3$), 3.03 (m, 2H, CH$_2$ of C*H*$_2$CH$_2$CH$_2$NH), 2.89 (m, 1H, CH$_2$ of Tyr), 2.70 (m, 1H, CH$_2$ of Tyr), 1.69 (m, 1H, CH$_2$CH$_2$C*H*$_2$NH), 1.54 (m, 1H, CH$_2$CH$_2$C*H*$_2$NH), 1.45 (m, 2H, CH$_2$ of CH$_2$CH$_2$CH$_2$NH), 1.43 ppm (s, 9H, Boc C(C*H*$_3$)$_3$); ^{13}C{^{1}H} NMR ([D$_6$]DMSO): $\delta = 172.6$, 171.8, 170.4, 169.9, 168.9, 157.4, 153.5, 137.7, 130.7, 130.3, 128.9, 128.2, 128.1, 114.8, 89.6, 76.9, 70.7, 69.5, 69.4, 65.9, 61.4, 45.3, 52.4, 52.2, 42.3, 37.2, 31.4, 28.6, 28.5, 22.5, 14.4 ppm; FTIR (KBr): $\tilde{\nu} = 3301$ (m, N-H), 1741 cm^{-1} (s, C=O); TOF-MS: *m*/*z*: calcd for $C_{43}H_{53}N_9O_{11}Fe$: 927.3214; found: 927.3217 $[M]^+$.

Thc-Fca-Gly-Gly-Tyr(Bz)-Arg(NO$_2$)-OMe (3): After the removal of the Boc group from **2** (1.1 mmol, 1.01 g) using TFA (1.5 mL), the excess acid was removed in vacuo and Et_3N (1.0 mL) in CH_2Cl_2 (10 mL) was added. To this was added a solution of Thc-OBt, prepared in situ from thiostic-OH (1.0 mmol, 0.206 g), HOBt (1.1 mmol, 0.153 g), and EDCI·HCl (1.1 mmol, 0.191 g) in dry CH_2Cl_2 (15 mL, 0 °C). The reaction mixture was then warmed to room temperature and left to stir overnight. The reaction mixture was then treated consecutively with aqueous solutions of $NaHCO_3$ (sat.), citric acid (10%), and water, dried over Na_2SO_4, and evaporated to dryness under reduced pressure. The crude product was purified by flash column chromatography (silica gel, EtOAc/MeOH 95:5) to give pale yellow crystals of compound **3** (0.69 g, 68%). ^{1}H NMR ([D$_6$]DMSO): $\delta = 8.38$ (s, 1H, NH), 8.36 (s, 1H, NH), 8.10 (br s, 2H, NH), 8.04 (br s, 2H, NH), 7.43 (d, 2H, $J = 7$ Hz, Bz), 7.38 (t, 2H, $J =$ 9 Hz, Bz), 7.32 (t, 1H, $J = 9$ Hz, Bz), 7.15 (d, 2H, $J = 8$ Hz, Tyr-Bz), 6.90 (d, 2H, $J = 8$ Hz, Tyr-Bz), 5.06 (s, 2H, Tyr(O-CH$_2$)), 4.78 (s, 2H, H-2, H-5, Fc), 4.58 (s, 2H, H-2′, H-5′, Fc), 4.44 (1H, m, Tyr αH), 4.42 (s, 2H, H-3, H-4, Fc), 4.26 (m, 1H, Arg αH), 4.05 (s, 2H, H-3′, H-4′, Fc), 3.96 (s, 2H, Gly^{1}αH), 3.66 (s, 2H, Gly^{2}αH), 3.64 (s, 3H, COOCH$_3$), 3.61 (m, 1H, CH$_2$ of Thc), 3.20 (m, 1H, CH$_2$ of Thc), 3.14 (m, 1H, CH$_2$ of Thc), 3.03 (m, 2H, CH$_2$ of C*H*$_2$CH$_2$CH$_2$NH), 2.89 (m, 1H, CH$_2$ of Tyr), 2.70 (m, 1H, CH$_2$ of Tyr), 2.49 (m, 1H, CH$_2$ of Thc), 2.30 (m, 2H, Thc (CH$_2$)), 1.90 (m, 1H, Thc (CH)), 1.75 (m, 4H, two CH$_2$ of Thc), 1.69 (m, 1H, CH$_2$ of CH$_2$CH$_2$C*H*$_2$NH), 1.54 (m, 1H, CH$_2$ of CH$_2$CH$_2$C*H*$_2$NH), 1.53 (m, 2H, Thc (CH$_2$)), 1.45 ppm (m, 2H, CH$_2$ of CH$_2$CH$_2$CH$_2$NH); ^{13}C{^{1}H} NMR ([D$_6$]DMSO): $\delta = 172.6$, 171.8, 171.4, 170.6, 169.7, 168.9, 157.4, 137.7, 130.6, 130.2, 128.8, 128.2, 128.1, 114.8, 97.1, 77.0, 71.7, 69.6, 69.6, 69.4, 66.0, 62.2, 65.6, 54.4, 52.4, 52.2, 42.7, 42.3, 38.6, 37.2, 36.2, 34.7, 34.6, 28.8, 28.7, 28.4, 25.3, 24.7 ppm; FTIR (KBr): $\tilde{\nu} = 3297$ (br m, N-H), 1741, 1653, 1538 cm^{-1} (s, C=O); TOF-MS; *m*/*z*: calcd for $C_{46}H_{57}O_{10}N_9S_2Fe$: 1015.3019; found: 1015.3025 $[M]^+$.

Fca-Gly-Gly-Tyr(Bz)-Arg(NO$_2$)-OH (4): A solution of 1N NaOH in water (2.6 mL) was added while stirring to a solution of compound **3** (0.50 g, 0.49 mmol) in MeOH (2.0 mL). The reaction was stored at room temperature for 6 h after which 1N HCl (1.5 mL) was added. The MeOH was then removed in vacuo followed by cooling of the solution in a ice bath prior to the dropwise addition of 1N HCl (3.0 mL). The solution was then stored in the fridge for 3 h after which the precipitate was filtered off and washed three times with cold, distilled water (50 mL) and dried under reduced pressure overnight to give compound **4** as a yellow solid (0.69 g, 68%). M.p. 152–159 °C; ^{1}H NMR ([D$_6$]DMSO): $\delta = 9.44$ (s, 1H, COOH), 8.63 (s, 1H, NH), 8.29 (s, 1H, NH), 8.22 (s, 1H, NH), 8.12 (br s, 2H, NH), 7.36 (br s, 1H, NH), 7.42 (d, 2H, $J = 8$ Hz, Bz), 7.38 (t, 2H, $J = 9$ Hz, Bz), 7.32 (t, 1H, $J = 8$ Hz, Bz), 7.15 (d, 2H, $J = 9$ Hz, Tyr-Bz), 6.90 (d, 2H, $J = 9$ Hz, Tyr-Bz), 5.06 (s, 2H, Tyr(O-CH$_2$)), 4.78 (s, 2H, H-2, H-5, Fc), 4.58 (s, 2H, H-2′, H-5′, Fc), 4.44 (m, 1H, Tyr αH), 4.42 (s, 2H, H-3, H-4, Fc), 4.26 (m, 1H, Arg αH), 4.05 (s, 2H, H-3′, H-4′, Fc), 3.96 (s, 2H, Gly^{1}αH), 3.66 (s, 2H, Gly^{2}αH), 3.61 (m, 1H, CH$_2$ of Thc), 3.20 (m, 1H, CH$_2$ of Thc), 3.14 (m, 1H, CH$_2$ of Thc), 3.03 (m, 2H, CH$_2$

of $CH_2CH_2CH_2NH$), 2.89 (m, 1H, CH_2 of Tyr), 2.70 (m, 1H, CH_2 of Tyr), 2.49 (m, 1H, CH_2 of Thc), 2.30 (m, 2H, Thc CH_2), 1.90 (m, 1H, Thc CH), 1.75 (m, 4H, 2 CH_2 of Thc), 1.69 (m, 1H, CH_2 of $CH_2CH_2CH_2NH$), 1.54 (m, 1H, CH_2 of $CH_2CH_2CH_2NH$), 1.53 (m, 2H, Thc CH_2), 1.45 ppm (m, 2H, CH_2 of $CH_2CH_2CH_2NH$); $^{13}C\{^1H\}$ NMR ([D$_6$]DMSO): δ = 188.5, 171.4, 169.6, 159.8, 157.4, 137.7, 130.7, 128.9, 128.2, 114.8, 97.2, 77.1, 71.6, 69.6, 69.5, 65.9, 62.3, 56.6, 42.6, 38.6, 36.2, 43.7, 28.8, 25.4 ppm; FTIR (KBr): $\tilde{\nu}$ = 3297 (br m, N-H), 1741, 1654, 1546 cm^{-1} (s, C=O); TOF-MS: *m/z*: calcd for $C_{45}H_{55}O_{10}N_9S_2Fe$: 1001.2863; found: 1001.2865 $[M]^+$.

Boc-Arg(Mtr)-Tyr-OMe (5): Boc-Arg(Mtr)-OH (4.11 mmol, 2.00 g), HOBt (4.52 mmol, 0.75 g), and EDCI·HCl (4.52 mmol, 0.95 g) were mixed in dry CH_2Cl_2 (30 mL, 0 °C) and allowed to stirred for 30 min. To this, a solution of H-Tyr-OMe, obtained by treatment of H-Tyr-OMe·HCl (4.52 mmol, 1.14 g) with Et_3N (1.5 mL) in dry CH_2Cl_2 (20 mL) was added and the stirring continued at room temperature. The reaction mixture was then treated consecutively with aqueous solutions of saturated $NaHCO_3$, citric acid (10%), again saturated $NaHCO_3$ and water, dried over Na_2SO_4, filtered and evaporated to dryness under reduced pressure. The crude product was purified by flash column chromatography (silica gel, EtOAc/hexane 1:2) to give compound **5** as a white crystalline solid (2.32 g, 85%). ^1H NMR ($CDCl_3$): δ = 7.48 (s, 1H, Bz-OH), 6.97 (d, 2H, J=8 Hz, Tyr-Bz), 6.91 (br s, 1H, αNH Arg), 6.78 (d, 2H, J=8 Hz, Tyr-Bz), 6.55 (s, 1H, Ar-H (Mtr)), 6.20 (br s, 2H, NH of guanidine), 5.98 (br s, 1H, NH of guanidine group), 5.41 (br s, 1H, Boc NH), 4.79 (m, 1H, Arg αH), 4.00 (m, 1H, Tyr αH), 3.89 (s, 3H, $COOCH_3$), 3.75 (s, 3H, OCH_3 of Mtr), 3.15 (m, 2H, CH_2 of $CH_2CH_2CH_2NH$), 3.09 (m, 1H, CH_2 of Tyr), 2.88 (m, 1H, CH_2 of Tyr), 2.70 (s, 3H, Ar-CH_3 of Mtr), 2.62 (s, 3H, Ar-CH_3 of Mtr), 2.14 (s, 3H, Ar-CH_3 of Mtr), 1.54 (m, 2H, CH_2 of $CH_2CH_2CH_2NH$), 1.42 (s, 9H, Boc C(CH_3)$_3$), 1.23 ppm (m, 2H, CH_2 of $CH_2CH_2CH_2NH$); TOF-MS: *m/z*: calcd for $C_{31}H_{45}O_9N_5S$: 663.2938; found: 663.2940 $[M]^+$.

Boc-Gly-Gly-Arg(Mtr)-Tyr-OMe (6): Boc-Arg(Mtr)-Tyr-OMe (3.01 mmol, 2.00 g) was dissolved in CH_2Cl_2 (3 mL) and treated with TFA (3 mL) for 30 min. The CH_2Cl_2 and TFA were subsequently removed in vacuo. The resulting residue was redissolved in CH_2Cl_2 (10 mL) and cooled in an ice bath prior to the dropwise addition of Et_3N (1.2 mL). To this was added a solution of Boc-Gly-Gly-OBt, prepared in situ from Boc-Gly-Gly-OH (2.74 mmol, 0.64 g), HOBt (3.0 mmol, 0.46 g), and EDCI·HCl (3.0 mmol, 0.58 g) in dry CH_2Cl_2 (20 mL, 0 °C). The reaction mixture was then warmed to room temperature and left to stir overnight. The resulting solution was then treated as per **5**. The product was purified by flash column chromatography (silica gel, EtOAc/hexane 1:2) and recrystallized from $CHCl_3$ to yield white crystalline compound **6** (1.73 g, 74%). ^1H NMR ([D$_6$]DMSO): δ = 9.22 (s, 1H, Bz-OH), 8.42 (s, 1H, NH-C(NH)-NH(Mtr), 8.30 (d, 1H, J=6 Hz, αNH(Arg), 8.09 (s, 1H, NH of guanidine group), 8.05 (s, 1H, NH of guanidine group), 7.96 (d, 1H, J=6 Hz, αNH(Tyr), 6.97 (d, 2H, J=8 Hz, Tyr-Bz), 6.68 (s, 1H, Ar-H of Mtr), 6.64 (d, 2H, J=8 Hz, Tyr-Bz), 6.38 (br s, 2H, NH of guanidine group), 4.60 (m, 1H, Tyr αH), 4.30 (m, 1H, Arg αH), 3.82 (d, 2H, Gly αH), 3.78 (s, 3H, $COOCH_3$), 3.70 (d, 2H, Gly αH), 3.53 (s, 3H, OCH_3 of Mtr), 3.01 (m, 2H, CH_2 of $CH_2CH_2CH_2NH$), 2.88 (m, 1H, CH_2 of Tyr), 2.82 (m, 1H, CH_2 of Tyr), 2.59 (3H, s, Ar-CH_3 of Mtr), 2.49 (s, 3H, Ar-CH_3 of Mtr), 2.04 (s, 3H, Ar-CH_3 of Mtr), 1.62 (m, 1H, CH_2 of $CH_2CH_2CH_2NH$), 1.43 (s, 9H, Boc C(CH_3)$_3$), 1.36 (m, 2H, CH_2 of $CH_2CH_2CH_2NH$), 1.23 ppm (m, 1H, CH_2 of $CH_2CH_2CH_2NH$); $^{13}C\{^1H\}$ NMR ([D$_6$]DMSO): δ = 172.3, 171.9, 170.2, 168.9, 1579, 156.6, 156.5, 156.3, 138.1, 136.1, 130.6, 130.5, 127.5, 115.5, 112.2, 78.6, 56.0, 54.5, 52.3, 52.2, 52.1, 43.7, 42.3, 63.4, 28.7, 24.1, 22.5, 18.5, 12.2 ppm; TOF-MS: *m/z*: calcd for $C_{35}H_{51}O_{11}N_7S$: 777.3367; found: 777.3370 $[M]^+$.

Boc-Fca-Gly-Gly-Arg(Mtr)-Tyr-OMe (7): Boc-Gly-Gly-Arg(Mtr)-Tyr-OMe (1.9 mmol, 1.50 g) was dissolved in CH_2Cl_2 and treated with TFA (2 mL) in CH_2Cl_2 (2 mL) for 30 min. The TFA and CH_2Cl_2 were subsequently removed in vacuo. The resulting residue was re-dissolved in CH_2Cl_2 and cooled in ice bath prior to the dropwise addition of Et_3N (0.50 mL). To this was added a solution of Boc-Fca-OBt (1.73 mmol, 0.80 g). The reaction mixture was then warmed to room temperature and left to stir overnight. The residue was purified by chromatography ($CHCl_3$/MeOH 90:10) to give compound **7** as a yellow solid (1.47 g, 85%). ^1H NMR ([D$_6$]DMSO): δ = 9.22 (s, 1H, Bz-OH), 8.42 (1H, s, NH of guanidine group), 8.30 (d, 1H, J=6.3 Hz, αNH Arg), 8.09 (s, 1H, NH of guanidine group), 8.05 (s, 1H, NH of guanidine group), 7.96 (d, 1H, J=6 Hz, αNH Tyr), 6.97 (d, 2H, J=8 Hz, Tyr-Bz), 6.68 (s, 1H, Ar-H of Mtr), 6.64 (d, 2H, J=8 Hz, Tyr-Bz), 6.38 (br s, 2H, NH of guanidine group), 4.72 (s, 2H, H-2, H-5, Fc), 4.60 (m, 1H, Tyr αCH), 4.47 (s, 2H, H-2′, H-5′, Fc), 4.30 (m, 1H, Arg αCH), 4.24 (s, 2H, H-3, H-4, Fc), 3.95 (s, 2H, H-3′, H-4′, Fc), 3.82 (d, 2H, αCH_2 Gly αCH_2), 3.78 (s, 3H, $COOCH_3$), 3.70 (d, 2H, Gly αCH_2), 3.53 (s, 3H, OCH_3(Mtr)), 3.01 (m, 2H, CH_2 of $CH_2CH_2CH_2NH$), 2.88 (m, 1H, CH_2 of Tyr), 2.82 (m, 1H, CH_2 of Tyr), 2.59 (s, 3H, Ar-CH_3 of Mtr), 2.49 (s, 3H, Ar-CH_3 of Mtr), 2.04 (s, 3H, Ar-CH_3 of Mtr), 1.62 (m, 1H, CH_2 of $CH_2CH_2CH_2NH$), 1.43 (9H, s, Boc C(CH_3)$_3$), 1.36 (m, 2H, CH_2 of $CH_2CH_2CH_2NH$), 1.23 ppm (m, 1H, CH_2 of $CH_2CH_2CH_2NH$); $^{13}C\{^1H\}$ NMR ([D$_6$]DMSO): δ = 172.7, 172.4, 170.3, 170.0, 169.4, 157.9, 156.6, 153.5, 138.1, 138.1, 136.1, 130.5, 127.3, 124.0, 115.6, 112.2, 100.0, 79.7, 76.8, 71.7, 69.3, 65.8, 56.0, 5.3, 52.2, 42.9, 42.1, 36.5, 28.6, 24.1, 18.5, 12.2 ppm; TOF-MS: *m/z*: calcd for $C_{46}H_{60}O_{12}N_8SFe$: 1004.3401; found: 1004.3402 $[M]^+$.

Thc-Fca-Gly-Gly-Arg(Mtr)-Tyr-OMe (8): The Boc group was removed from compound **7** (1.2 mmol, 1.20 g) by addition of TFA (1.5 mL). After 30 min, the excess acid was removed in vacuo and Et_3N (0.7 mL) in CH_2Cl_2 (10 mL) was added. To this was added a solution of Thc-OH (1.1 mmol, 0.224 g), HOBt (1.2 mmol, 0.184 g), and EDCI·HCl (1.2 mmol, 0.230 g) in dry CH_2Cl_2 (15 mL, 0 °C). The reaction mixture was left to stir overnight at room temperature and then treated to an aqueous work up as described above. The crude product was purified by flash column chromatography (silica gel, EtOAc/MeOH 90:10) to give a pale yellow solid of compound **8** (0.89 g, 68%). ^1H NMR ([D$_6$]DMSO): δ = 9.22 (s, 1H, Bz-OH), 8.42 (s, 1H, NH of guanidine group), 8.30 (d, 1H, J=6 Hz, αNH Arg), 8.09 (s, 1H, NH of guanidine group), 8.0 (s, 1H, NH of guanidine group), 7.96 (d, 1H, J=6 Hz, αNH Tyr), 6.97 (d, 2H, J=8 Hz, Tyr-Bz), 6.68 (s, 1H, Ar-H of Mtr), 6.64 (d, 2H, J=8 Hz, Tyr-Bz), 6.38 (br s, 2H, NH of guanidine group), 4.72 (s, 2H, H-2,m H-5, Fc), 4.60 (1H, m, Tyr αH), 4.47 (s, 2H, H-2′, H-5′, Fc), 4.30 (1H, m, Arg αH), 4.24 (s, 2H, H-3, H-4, Fc), 3.95 (s, 2H, H-3′, H-4′, Fc), 3.82 (d, 2H, Gly αH_2), 3.78 (s, 3H, $COOCH_3$), 3.70 (d, 2H, Gly αH_2), 3.61 (m, 1H, CH_2 of Thc), 3.53 (s, 3H, OCH_3 of Mtr), 3.20 (m, 1H, CH_2 of Thc), 3.14 (m, 1H, CH_2 of Thc), 3.01 (m, 2H, CH_2 of $CH_2CH_2CH_2NH$), 2.88 (m, 1H, CH_2 of Tyr), 2.82 (m, 1H, CH_2 of Tyr), 2.59 (s, 3H, Ar-$CH_3$of Mtr), 2.49 (m, 1H, CH_2 of Thc), 2.49 (s, 3H, Ar-CH_3 of Mtr), 2.30 (2H, m, Thc CH_2), 1.90 (m, 1H, Thc (CH)), 2.04 (s, 3H, Ar-CH_3 of Mtr), 1.75 (m, 4H, two CH_2 of Thc), 1.62 (m, 1H, CH_2 of $CH_2CH_2CH_2NH$), 1.53 (m, 2H, Thc (CH_2)), 1.36 (m, 2H, CH_2 of $CH_2CH_2CH_2NH$), 1.23 ppm (m, 1H, CH_2 of $CH_2CH_2CH_2NH$); $^{13}C\{^1H\}$ NMR ([D$_6$]DMSO): δ = 188.5, 172.2, 172.1, 171.9, 171.4, 170.6, 169.8, 169.0, 157.9, 156.6, 149.6, 138.1, 136.1, 135.0, 124.0, 122.0, 112.2, 97.1, 79.7, 77.0, 71.7, 69.4, 66.0, 62.2, 56.5, 56.5, 56.0, 52.3, 38.6, 34.7, 34.5, 25.3, 24.6, 24.1, 12.2 ppm; FTIR (KBr): $\tilde{\nu}$ = 3315, 3090 (br m, N-H), 1722, 1655, 1548 cm^{-1} (s, C=O); TOF-MS: *m/z*: calcd for $C_{49}H_{64}O_{11}N_8S_3Fe$: 1092.3206; found: 1092.3208 $[M]^+$.

Thc-Fca-Gly-Gly-Arg(Mtr)-Tyr-OH (9): Methyl ester **8** (0.20 g, 0.18 mmol) was deprotected as described for compound **4** to give free acid **9** as a yellow solid (0.16 g, 82%). M.p. 125–133 °C; ^1H NMR ([D$_6$]DMSO): δ = 9.58 (s, 1H, COOH), 9.05 (s, 1H, Tyr-OH), 8.49 (s, 1H, NH of guanidine group), 8.35 (d, 1H, J=6 Hz, αNH Arg), 8.18 (s, 1H, NH of guanidine group), 8.05 (s, 1H, NH of guanidine group), 7.95 (d, 1H, J=6 Hz, αNH(Tyr)), 7.59 (1H, m, αNH(Gly)), 7.25 (m, 1H, αNH(Gly)), 6.94 (2H, d, J=8 Hz, Tyr-Bz), 6.67 (s, 1H, Ar-H of Mtr), 6.57 (2H, d, J=8 Hz, Tyr-Bz), 4.75 (d, 2H, J=9 Hz, H-2, H-5, Fc), 4.60 (m, 1H, Arg αH), 4.59 (d, 2H, J=9 Hz, H-2′, H-5′, Fc), 4.24 (s, 2H, H-3, H-4, Fc), 4.17 (m, 1H, Tyr αH), 3.97 (s, 2H, H-3′, H-4′, Fc), 3.84 (d, 2H, Gly αCH_2), 3.84 (s, 3H, Ar-O-CH_3 of Mtr), 3.75 (d, 2H, Gly αCH_2), 3.61 (m, 1H, CH_2 of Thc), 3.53 (s, 3H, OCH_3 of Mtr), 3.17 (m, 1H, CH_2 of Thc), 3.11 (m, 1H, CH_2 of Thc), 2.97 (m, 2H, CH_2 of $CH_2CH_2CH_2NH$), 2.88 (m, 1H, CH_2 of Tyr), 2.82 (m, 1H, CH_2 of Tyr), 2.60 (s, 3H, Ar-CH_3 of Mtr), 2.49 (m, 1H, CH_2 of Thc), 2.49 (s, 3H, Ar-CH_3 of Mtr), 2.30 (m, 2H, Thc CH_2), 1.91 (m, 1H, Thc CH), 2.04 (s, 3H, Ar-CH_3 of Mtr), 1.74 (m, 4H, two CH_2 of Thc), 1.60 (m, 1H, CH_2 of $CH_2CH_2CH_2NH$), 1.53 (m, 2H, Thc CH_2), 1.36 (m, 2H, CH_2 of $CH_2CH_2CH_2NH$), 1.22 (m, 1H,

CH_2 of $CH_2CH_2CH_2NH$), 0.85 ppm (m, 1H, CH_2 of $CH_2CH_2CH_2NH$); $^{13}C\{^1H\}$ NMR ([D$_6$]DMSO): δ = 188.5, 172.2, 172.1, 171.9, 171.4, 170.6, 169.8, 169.0, 157.9, 156.6, 149.6, 138.1, 136.1, 135.0, 124.0, 122.0, 112.2, 97.1, 79.7, 77.0, 71.7, 69.4, 66.0, 62.2, 56.5, 56.5, 56.0, 52.3, 38.6, 34.7, 34.5, 25.3, 24.6, 24.1, 12.2 ppm; FTIR (KBr): $\tilde{\nu}$ = 3306, 3086 (m, N-H), 1748 (s, C=O), 1656 (amide I), 1550 cm^{-1} (amide II); TOF-MS: m/z: calcd for $C_{48}H_{62}O_{11}N_8S_3Fe$: 1078.3049; found: 1078.3049 $[M]^+$.

Thc-Fca-Gly-Gly-Arg-Tyr-OH (10): Thc-Fca-Gly-Gly-Arg(Mtr)-Tyr-OH (**9**) (60 mg, 0.07 mmol) was suspended in CH_2Cl_2 (2 mL) and a mixture (TFA/thioanisole/H_2O 96:3:1, 3 mL) was added and the mixture left to stir for 4 h at RT. The reaction mixture was concentrated in vacuo, the resulting residue was dissolved in TFA and precipitated by a dropwise addition to ice-cold Et_2O. The precipitate was collected by centrifugation, and purified by semi-preparative HPLC (t_R=22.4 min, λ=220 nm) to yield a faint yellow solid of compound **10** (22 mg, 0.03 mmol, 37%). RP-HPLC (analytical, t_R=9.8 min); m.p. 118–122 °C; ^{1}H NMR ([D$_6$]DMSO): δ = 9.48 (s, 1H, COOH), 9.23 (s, 1H, Tyr-OH), 8.30 (1H, m, αNH Arg), 8.22 (s, 1H, NH of guanidine group), 8.02 (1H, s, NH of guanidine group), 7.66 (m, 1H, αNH(Tyr), 7.56 (2H, m, αNH(Gly)), 6.93 (d, 2H, J=8 Hz, Tyr-Bz), 6.57 (2H, d, J=8 Hz, Tyr-Bz), 4.75 (s, 2H, H-2, H-5, Fc), 4.60 (s, 2H, H-2′, H-5′, Fc), 4.26 (m, 1H, Arg αH), 4.25 (s, 2H, H-3, H-4, Fc), 4.01 (m, 1H, Tyr αH), 3.98 (s, 2H, H-3′, H-4′, Fc), 3.80 (d, 2H, Gly αH_2), 3.77 (d, 2H, Gly αH_2), 3.61 (1H, m, CH_2 of Thc), 3.20 (m, 1H, CH_2 of Thc), 3.18 (1H, m, CH_2 of Thc),), 3.11 (m, 1H, CH_2 of Tyr), 2.98 (2H, m, CH_2 of C$H_2CH_2CH_2NH$), 2.83 (m, 1H, CH_2 of Tyr), 2.71 (2H, s, NH_2 of guanidine group), 2.41 (m, 2H, Thc CH_2), 2.36 (1H, m, CH_2 of Thc), 2.15 (m, 1H, CH_2 of Thc), 1.66 (2H, m, CH_2 of $CH_2CH_2CH_2NH$), 1.55 (m, 2H, Thc CH_2), 1.35 (m, 2H, CH_2 of $CH_2CH_2CH_2NH$), 1.23 (m, 1H, CH_2 of $CH_2CH_2CH_2NH$), 0.85 ppm (m, 1H, CH_2 of $CH_2CH_2CH_2NH$); $^{13}C\{^1H\}$ NMR ([D$_6$]DMSO): δ = 172.1, 172.0, 171.8, 171.4, 170.5, 169.8, 157.8, 156.6, 138.1, 136.1, 135.0, 123.9, 121.9, 112.2, 97.1, 79.7, 76.9, 71.7, 69.4, 65.9, 62.2, 56.5, 56.4, 52.3, 38.5, 34.7, 34.5, 25.3, 24.6, 24.2 ppm; FTIR (KBr): $\tilde{\nu}$ = 3447 (m, N-H), 1725 (s, C=O), 1658 (amide I), 1547 cm^{-1} (amide II); TOF-MS: m/z: calcd for $C_{38}H_{50}O_8N_8S_2Fe$: 866.2542; found: 866.2541 $[M]^+$.

Papain inhibition studies: For the inhibition studies, the following stock solutions were prepared:

A 5 mM stock solution of the chromogenic substrate Z-Phe-Arg-NHNp was prepared in DMSO.

Stock solutions of the Fca–peptide inhibitors were prepared in DMSO.

A papain stock solution was prepared in 1 mM HCl. For daily activation, the papain stock solution was diluted 1:100 in 0.1 M sodium phosphate pH 6.5, containing 2.5 mM EDTA and 15 mM DTT and was incubated at 23 °C for 1 h. The activated enzyme was kept on ice.

Inhibition of papain enzyme was assayed at 23 °C with the chromogenic substrate Z-Phe-Arg-NHNp (200 μM) in the presence of increasing concentrations of the inhibitory peptides 4, 9 and 10. The buffer solution used for the assay was 0.1 M sodium phosphate pH 6.2, 2.5 mM EDTA, 300 μM DTT, and 30% DMSO. Rates were determined by duplicate measurements of seven different concentrations of each single inhibitor. The concentration of the liberated *p*-nitroaniline (*p*NA) was monitored spectrophotometrically by measuring the absorbance at λ=405 nm against a blank sample containing no enzyme and an extinction coefficient of ε=9.96 cm^2 μmol^{-1}. The final volume made up to 1 mL. The reaction was initiated by addition of the enzyme (20 μL); its final concentration catalyze the conversation of the substrate with a rate of 1–2 μM min^{-1}. Progress curves were monitored over 10 min. A control assay to determine the total hydrolysis of Z-Phe-Arg-NHNp (480 μM) was carried out in the absence of the inhibitors (70 μL DMSO was added to the cuvette). The papain concentration was 20-fold higher than the inhibition assays. The resulting activity was considered as 100%. A Lineweaver–Burk plot was constructed and the value of the Michaelis–Menten constant (K_m) was determined. The apparent inhibition constants K_i' were determined by fitting equation 3[26] to the experimental data.

$$\vartheta = \frac{\vartheta_0}{1 + [\mathrm{I}]/K_i'} \quad (3)$$

where ϑ is the rate, ϑ_0 is the rate in the absence of the inhibitor, [I] is the inhibitor concentration and K_i' is the apparent inhibition constant. The true inhibition constants K_i were calculated by correction of K_i' according to Equation (4)[26]

$$K_i = \frac{K_i'}{1 + [\mathrm{S}]/K_m} \quad (4)$$

where [S] is the substrate concentration and K_m is the Michaelis–Menten constant.

Preparation of peptide arrays: Peptide arrays on spot ready SPR chips were prepared by spotting three different peptides **4**, **9** and **10** on three arrays. The gold chip was placed on a piece of clean parafilm in a humidity chamber and the freshly prepared peptide solutions were spotted immediately 5 mM in DMSO (100 mM TEA pH 8) for 20 h. As a control experiment, a 5 mM solution of decanethiol was used to immobilize the decanethiol onto the control array. The excess probe solutions were then removed with a pipet prior to rinsing with the few mL of buffer solution (0.1 M sodium phosphate, pH 6.2, 2.5 mM EDTA, 300 μM DTT, and 30% DMSO, T=23±3 °C).

Preparation of films on flat substrates: Each peptide was immobilized on the gold surface of a plane SPR chip by soaking the chips overnight in a 1 mM solution of disulfide-terminated peptides **4**, **9** and **10** in dry ethanol.

Real-time SPR imaging studies: An SPR imaging system (GWC Technologies) was used for the real-time monitoring of the interaction between immobilized peptides and papain enzyme. Briefly, a collimated p-polarized light at a fixed angle reflected from the sample/gold/prism assembly was sent through a narrow band-pass filter and then detected with a CCD camera. The data were collected using the software package V++ (Digital Optics, NZ). Custom macros were used so that data could be collected with simultaneous processing of several specific user designated regions of interest (ROIs) on the array surface.[42] Kinetic data for each ROI were obtained by collecting one data point approximately every 1 s, which was the average of five camera frames. The difference in percent reflectivity for each probe area was normalized with respect to the average change in percent reflectivity measured for the buffer background. Kinetic data from multiple identical array elements were averaged to obtain the final SPR response curves. Microsoft Excel and Origin 7.5 were used for all data processing and kinetic model fitting in these experiments.

Surface electrochemistry: Peptide films were immobilized on home made 25 μm diameter microelectrodes by soaking the gold electrodes in 1 mM solution of disulfide terminated peptides for 36 h. Then, the concentrated film was diluted by immersing the modified electrodes in 1 mM ethanolic solution of decanethiol for 2 min. The CVs were recorded in aqueous solutions of $NaClO_4$ (2.0 M). Ag/AgCl was used as a pseudo-reference electrode, and Pt wire as a counter electrode. Ten gold microelectrodes with peptide films were measured for each compound and all experiments were carried out at room temperature (23±3 °C). Blocking studies were carried out in a solution containing 0.1 mM $[Ru(NH_3)_6Cl_3]$ and 0.1 N $HClO_4$, see Supporting Information, Figure S6.

Studies using the electrochemical quartz crystal microbalance: An EQCM system interfaced to a PC (CH instruments 440) was used for recording the frequency change during the process of protein adsorption onto the peptide film. The EQCM electrodes with a fundamental resonant frequency of 8 MHz and 13.7 mm diameter were of the AT-cut type, with optically polished surfaces coated on both sides with 200 nm thick gold layer, 5 mm diameter, over a thin chromium adhesion mediator film. Since the EQCM operated in time-resolved mode, the frequency difference of the working crystal and the reference crystal was measured. The relationship between the changes in mass per unit area (m) and frequency (f) are given by Sauerbrey equation [Eq. (5)]:[56]

$$\Delta f = \frac{-2\Delta m n f_0^2}{A\sqrt{\mu_q \pi_q}} \quad (5)$$

where A is the surface area of the electrode, μ_q is shear modulus of quartz and ρ_q is the density of quartz.

Acknowledgements

Financial support from NSERC is gratefully acknowledged. H.B.K. holds the Canada Research Chair in Biomaterials. We are grateful to the Saskatchewan Structure Science Center (SSSC) for providing access to all necessary instrumentation. Ken Thoms, Chemistry Department, University of Saskatchewan, is also acknowledged for carrying out the MALDI-TOF experiments.

[1] A. P. Turner, I. Karube, G. Wilson, in *Bionsensors: Fundamentals and Applications*, Oxford Science Publications, Oxford, **1986**, p. 770.
[2] J. Wang, *Analytical Electrochemistry*, 2ed ed., Wiley, New York, **2000**.
[3] L. Murphy, *Curr. Opin. Chem. Biol.* **2006**, *10*, 177–184.
[4] J. Wang, *Analyst* **2005**, *130*, 421–426.
[5] E. Bakker, Y. Qin, *Anal. Chem.* **2006**, *78*, 3965–3983.
[6] M. Mehrvar, M. Abdi, *Anal. Sci.* **2004**, *20*, 1113–1126.
[7] J. Wang, *Biosens. Bioelectron.* **2006**, *21*, 1887–1892.
[8] J. Wang, *J. Pharm. Biomed. Anal.* **1999**, *19*, 47–53.
[9] Y. Katayama, Y. Ohuchi, H. Higashi, Y. Kudo, M. Maeda, *Anal. Chem.* **2000**, *72*, 4671–4674.
[10] F. Le Floch, H. A. Ho, M. Leclerc, *Anal. Chem.* **2006**, *78*, 4727–4731.
[11] J. N. Barisci, D. Hughes, A. Minett, G. G. Wallace, *Anal. Chim. Acta* **1998**, *371*, 39–48.
[12] W. Lu, T. A. Nguyen, G. G. Wallace, *Electroanalysis* **1998**, *10*, 1101–1107.
[13] W. Lu, G. G. Wallace, A. A. Karayakin, *Electroanalysis* **1998**, *10*, 472–476.
[14] M. S. Wilson, W. Y. Nie, *Anal. Chem.* **2006**, *78*, 2507–2513.
[15] J. Liu, S. Tian, L. Tiefenauer, P. E. Nielson, W. Knoll, *anal. Chem.* **2005**, *77*, 2756–2761.
[16] C. Fan, K. W. Plaxco, A. J. Heeger, *Proc. Natl. Acad. Sci. USA* **2003**, *100*, 9134–9137.
[17] C. Fan, K. W. Plaxco, A. J. Heeger, *J. Am. Chem. Soc.* **2002**, *124*, 5642–5643.
[18] D. R. van Staveren, N. Metzler-Nolte, *Chem. Rev.* **2004**, *104*, 5931–5985.
[19] C. H. Devillers, D. Boturyn, C. Bucher, P. Dumy, P. Labbe, J.-C. Moutet, G. Royal, E. Saint-Aman, *Langmuir* **2006**, *22*, 8134–8143.
[20] C. Baldoli, C. Rigamonti, S. Maiorana, E. Licandro, L. Falciola, P. R. Mussini, *Chem. Eur. J.* **2006**, *12*, 4091–4100.
[21] H.-B. Kraatz, *J. Inorg. Organomet. Polym.* **2005**, *15*, 83–106.
[22] K. Plumb, H. B. Kraatz, *Bioconjugate Chem.* **2003**, *14*, 601–606.
[23] L. Barišić, M. Čakić, K. A. Mahmoud, Y. N. Liu, H. B. Kraatz, H. Pritzkow, S. I. Kirin, N. Metzler-Nolte, V. Rapić, *Chem. Eur. J.* **2006**, *12*, 4965–4980.
[24] L. Barisic, V. Rapić, N. Metzler-Nolte, *Eur. J. Inorg. Chem.* **2006**, 4019–4021.
[25] K. Heinze, U. Wild, M. Beckmann, *Eur. J. Inorg. Chem.* **2007**, 617–623.
[26] R. Loser, K. Schilling, E. Dimmig, M. Gutschow, *J. Med. Chem.* **2005**, *48*, 7688–7707.
[27] S. Blumberg, I. Schechte, A. Berger, *Eur. J. Biochem.* **1970**, *15*, 97–102.
[28] M. O. Funk, Y. Nakagawa, J. Skochdopole, E. T. Kaiser, *Int. J. Pept. Protein Res.* **1979**, *13*, 296–303.
[29] A. Albeck, S. Kliper, *Biochem. J.* **1997**, *322*, 879–884.
[30] M. J. Harrison, N. A. Burton, I. H. Hillier, *J. Am. Chem. Soc.* **1997**, *119*, 12285–12291.
[31] A. E. Howard, P. A. Kollman, *J. Med. Chem.* **1988**, *31*, 1669–1675.
[32] I. Schechter, A. Berger, *Papain Biochem. Biophys. Res. Commun.* **1967**, *27*, 157–162.
[33] A. Hall, M. Abrahamson, A. Grubb, J. Trojnar, P. Kania, R. Kasprzykowska, F. Kasprzykowski, *J. Enzyme Inhib.* **1992**, *6*, 113–123.
[34] Z. Grzonka, E. Jankowska, F. Kasprzykowski, R. Kasprzykowska, L. Lankiewicz, W. Wiczk, E. Wieczerzak, J. Ciarkowski, P. Drabik, R. Janowski, M. Kozak, M. Jaskolski, A. Grubb, *Acta Biochim. Pol.* **2001**, *48*, 1–20.
[35] R. Janowski, M. Kozak, E. Jankowska, Z. Grzonka, M. Jasko′ lski, *J. Pept. Res.* **2004**, *64*, 141–150.
[36] D. Yamamoto, K. Matsumoto, H. Ohishi, T. Ishida, M. Inoue, K. Kitamura, H. Mizuno, *J. Biol. Chem.* **1991**, *266*, 14771–14777.
[37] K. Matsumoto, M. Murata, S. Sumiya, K. Mizoue, K. Kitamura, T. Ishida, *Biochim. Biophys. Acta* **1998**, *1383*, 93–100.
[38] A. Pedretti, L. Villa, G. Vistoli, *J. Mol. Graphics Modell.* **2002**, *21*, 47–49.
[39] T. T. Goodrich, A. W. Wark, R. M. Corn, H. J. Lee, *Methods Mol. Biol.* **2006**, *328*, 113–130.
[40] S. O. Jung, H.-S. Ro, B. H. Kho, Y.-B. Shin, M. G. Kim, B. H. Chung, *Proteomics* **2005**, *5*, 4427–4431.
[41] G. J. Wegner, H. J. Lee, R. M. Corn, *Anal. Chem.* **2002**, *74*, 5161–5168.
[42] G. J. Wegner, A. W. Wark, H. J. Lee, E. Codner, T. Saeki, S. Fang, R. M. Corn, *Anal. Chem.* **2004**, *76*, 5677–5684.
[43] B. P. Nelson, T. E. Grimsrud, M. R. Liles, R. M. Goodman, R. M. Corn, *Anal. Chem.* **2001**, *73*, 1–7.
[44] P. R. Connelly, R. Varadarajan, J. M. Sturtevant, F. M. Richards, *Biochemistry* **1990**, *29*, 6108–6114.
[45] J. M. Goldberg, R. L. Baldwin, *Proc. Natl. Acad. Sci. USA* **1999**, *96*, 2019–2024.
[46] R. P. Hearn, F. M. Richards, J. Sturtevant, G. D. Watt, *Biochemistry* **1971**, *10*, 806–817.
[47] S. H. Park, R. T. Raines, *Protein Sci.* **1997**, *6*, 2344–2349.
[48] H. A. Biebuyck, C. D. Bian, G. M. Whitesides, *Langmuir* **1994**, *10*, 1825–1831.
[49] T. M. Willey, A. L. Vance, C. Bostedt, T. van Buuren, R. W. Meulenberg, L. J. Terminello, C. S. Fadley, *Langmuir* **2004**, *20*, 4939–4944.
[50] J. C. Miller, J. N. Miller, in *Ellis Horwood Series in Analytical Chemistry* (Eds.: R. A. Chalmers, M. Masson), Chichester, **1993**, p. 119.
[51] W. U. Dittmer, A. Reuter, F. C. Simmel, *Angew. Chem.* **2004**, *116*, 3634–3637; *Angew. Chem. Int. Ed.* **2004**, *43*, 3550–3553.
[52] J. W. Li, X. H. Fang, W. H. Tan, *Biochem. Biophys. Res. Commun.* **2002**, *292*, 31–40.
[53] R. F. Macaya, P. Schultze, F. W. Smith, J. A. Roe, J. Feigon, *Proc. Natl. Acad. Sci. USA* **1993**, *90*, 3745–3749.
[54] Y. Xiao, A. A. Lubin, A. J. Heeger, K. W. Plaxco, *Angew. Chem.* **2005**, *117*, 5592–5595; *Angew. Chem. Int. Ed.* **2005**, *44*, 5456–5459.
[55] K. A. Mahmoud, Y. T. Long, G. Schatte, H. B. Kraatz, *Eur. J. Inorg. Chem.* **2005**, 173–180.
[56] G. Sauerbrey, *Z. Phys.* **1959**, *155*, 206–222.

Received: December 24, 2006
Published online: April 23, 2007

